KAWASAKI STEEL TECHNICAL REPORT
No.5 (May 1982)

Beam Blank Deformation Characteristics during Open Pass Web Rolling

Takashi Kusaba, Toru Sasaki

Synopsis :
As an approach to clarifying complicated beam blank deformation characteristics during the open pass breakdown rolling into H-shapes, the deformation of dog bone beam blanks is studied using plasticine models starting with the web portion deformation behavior which is assumed to correspond to that of a flat plate under rolling force. Based on experimental results, mathematical expressions that can calculate the exact amount of metal flow and dimensions have been established to a level applicable to actual steel rolling. A new method of partial web rolling is also introduced.

The body can be viewed from the next page.

Beam Blank Deformation Characteristics during Open Pass Web Rolling*

Takashi KUSABA** Toru SASAKI**

As an approach to clarifying complicated beam blank deformation characteristics during the open pass breakdown rolling into H-shapes, the deformation of dog bone beam blanks is studied using plasticine models starting with the web portion deformation behavior which is assumed to correspond to that of a flat plate under rolling force. Based on experimental results, mathematical expressions that can calculate the exact amount of metal flow and dimensions have been established to a level applicable to actual steel rolling. A new method of partial web rolling is also introduced.

1 Introduction

The beam blank for large H-shapes is ordinarily formed by a two-high breakdown rolling mill provided with an open pass. In the rolling by an open pass, the rolling reduction at each portion of the cross section of material in the transverse direction is remarkably uneven, and in addition, different deformation elements act on one another, so that the metal flow is very complicated[1]. Therefore, the deformation behaviors in open pass rolling have hardly been analyzed.

The authors presume that, as a means of elucidating these complicated metal flow behaviors, it is effective from a practical point of view to decompose them into basic deformation elements and reconstitute them again after comprehending their deformation characteristics.

In this report, thus, the authors take up the case of web rolling from among basic deformation elements in the open pass rolling of beam blanks. This is because it is presumed that the deformation caused by the ordinary open pass rolling of beam blanks is substantially governed by the deformation of the web portion under direct reduction. First the deformation behavior[2] in the rolling of the web from which the flange is separated, namely, in plate rolling, and then the deformation behavior in the method of rolling only the web part[3] of beam blanks are analyzed by means of plasticine models. On the basis of the experimental results, expressions for estimating the amount of metal flow and external dimensions are prepared, and it is ascertained that these expressions have high accuracy and are sufficiently applicable to actual steel rolling. In addition, the partial web rolling method which is effective in rolling slabs into large H-shapes H700 × 300 – H900 × 300 is discussed to some extent.

2 Equation of Width Spread in Flat Plate Rolling

With the web portion assumed to be a plain flat plate, the deformation behavior in rolling by a flat roll was investigated.

2.1 Single Barrel Deformation

Assuming actual webs of beam blanks: H200 × 200, H400 × 200 and H600 × 200, flat plates having a shape factor (B_0/H_0, where B_0 stands for the original width of specimen and H_0 for the original thickness of specimen) of 1–4.5 were rolled to a rolling reduction range of 10%–40% on a gypsum roll of 300 mmϕ (scale: 1/5).

As shown in **Fig. 1**, the overall width after rolling was divided into the width (B_1) of the section in contact with the roll and the width of the swelled section (a) at both sides. It was ascertained that the shape of side swelling after flat rolling can be approximated as a quadratic curve. As a result, the mean width (B_{1m}) can be represented by equation **(1)**:

$$B_{1m} = \frac{4a + 3B_1}{3} \quad \cdots\cdots (1)$$

The width (B_1) of contact with the roll can be repre-

---

* Originally published in *Kawasaki Steel Giho*, **13** (1981) 3, pp. 13–25

** Research Laboratories

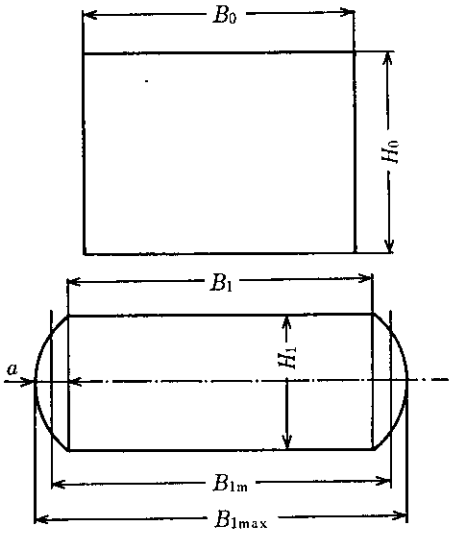

Fig. 1 Cross sections of plate before and after flat rolling

sented by the following equation obtained by modifying to some extent Yanagimoto's formula[4] on the basis of the experimental results:

$$B_1/B_0 = (H_0/H_1)^{0.395^{1.77}}$$

$$S = \frac{2\sqrt{R(H_0 - H_1)}}{H_0 + 2B_0} \quad \cdots\cdots\cdots\cdots\cdots\cdots (2)$$

Here, suffixes 0 and 1 stand for the conditions before and after rolling, respectively, and R for the radius of the roll.

The amount of swelling (a) on both sides can be represented by the following equation, through regression analysis in consideration of the influence of rolling conditions upon it:

$$2a/H_0 = 0.15\frac{\sqrt{\frac{2R}{H_0}}(H_0 - H_1)}{H_0 + B_0/5} \quad \cdots\cdots\cdots (3)$$

From eqs. **(1)**, **(2)** and **(3)**, eq. **(4)** can be derived as the mean spread ratio (B_{1m}/B_0):

$$B_{1m}/B_0 = (H_0/H_1)^{0.395^{1.77}} + \frac{0.1H_0(H_0 - H_1)\sqrt{\frac{2R}{H_0}}}{B_0(H_0 + B_0/5)} \quad \cdots\cdots\cdots\cdots (4)$$

Here, the amount of metal flow ΔM_S (where suffix S stands for a single barrel) is defined as eq. **(5)** as the cross section of the part protruding out of the plate width before rolling:

$$\Delta M_S = (B_{1m} - B_0)H_1 \quad \cdots\cdots\cdots\cdots\cdots\cdots (5)$$

2.2 Double Bulge Deformation

With the roll factor ($2R/H_0$) and the rolling reduction identical with those in Par. 2.1, a plate with shape factor of 0.18–1.1 was rolled. The ratio $\Delta M_S/\Delta S$, namely the amount of spread ΔM_S defined by eq. **(5)** to the reduction of area ΔS {$= (B_0(H_0 - H_1))$} was calculated. On the other hand, assuming ΔM as the amount of metal flow obtained experimentally, its ratio to ΔS was taken in the same way to evaluate the correspondence between them. The result showed that the measured values were much less than the calculated values, as shown by mark ● in **Fig. 2** and differed from the single barrel (marked ○, where the

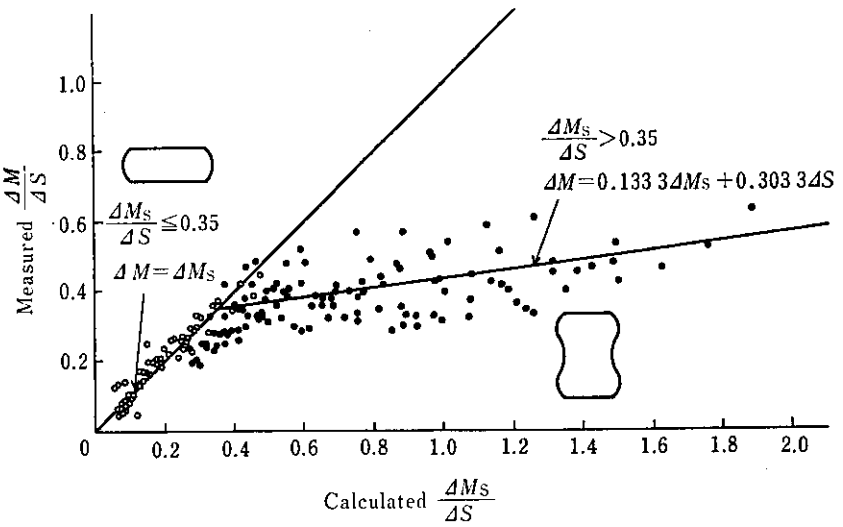

ΔM : Amount of metal flow, ΔS : Reduction of area

Fig. 2 Comparison between calculated $\Delta M_S/\Delta S$ andmeasured $\Delta M/\Delta S$ for both singlebarrel (○) and double bulge (●) deformation

calculated values correspond well with the measured values) shown at the same time. Therefore, eq. **(5)** cannot be used in the case of double bulge deformation which is likely to happen if the shape factor is small, and therefore it has to be changed into a linear equation to be obtained from **Fig. 2**. That is, when $\Delta M_S/\Delta S$ is more than 0.35, the amount of metal flow can be represented by eq. **(6)**. (Suffix D stands for double bulge.)

$$\Delta M_D = 0.133\,3\Delta M_S + 0.303\,3\Delta S$$
$$(\Delta M_S/\Delta S > 0.35) \cdots\cdots\cdots\cdots\cdots\cdots (6)$$

Thus, the amount of metal flow of plates having a wide range of shapes can be dealt with extensively by eq. **(5)** or **(6)**.

2.3 Estimation Accuracy of the Amount of Metal Flow

The comparison between the amount of metal flow calculated by eqs. **(5)** and **(6)** and the measured amount of metal flow is shown in **Fig. 3**. Mark ○ in the figure stands for single barrel deformation, and mark ● for double bulge deformation; in both, the estimation accuracy is considerably good.

3 Metal Flow Equation When a Plate is Non-homogeneously Rolled in Transverse Direction

As shown in **Fig. 4**, the web shape of an open pass greatly differs from that in the above-mentioned flat plate rolling in that the rolling reduction at both ends is less than that at the center, since the gap at both ends is larger than that at the center. Therefore, the spread under these conditions was investigated. In **Fig. 4**, the solid line represents the roll, the dotted line the cross section of material, and B_r stands for the length of the flattened part of the roll. As for the shape of the roll used, B_r was changed to 3 stages of 12 mm, 34 mm and 72 mm, so that the taper at both ends might be constantly 8/15.

3.1 Characteristic Deformation Behavior

A plasticine plate with at stripe pattern in its cross section was rolled by the three types of rolls mentioned above, and the post-rolling states of the plasticine plate are shown in **Photo. 1**, and **Fig. 5** shows the transverse distribution of the spread ratio of each of these unit stripes at midsection.
(a') and (b') in **Photo. 1** and the dotted line in **Fig. 5** are the results of rolling of a flat plate having a width corresponding to the length of the flat part of the roll.

It is clear from **Photo. 1** and **Fig. 5** that the flat portion at the center of the material rolled non-homogeneously in transverse direction spreads larger in width direction than in the case of homogeneously

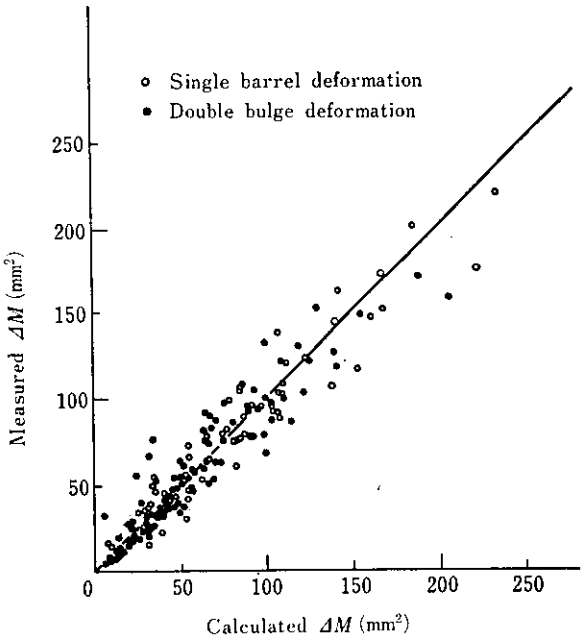

Fig. 3 Comparison between calculated and measured ΔM for plate rolling with the B_0/H_0 ratio from 0.18 to 4.5

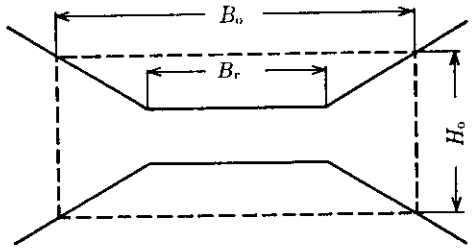

Fig. 4 Web part of pass rolls (solid line) and plate specimen (dotted line)

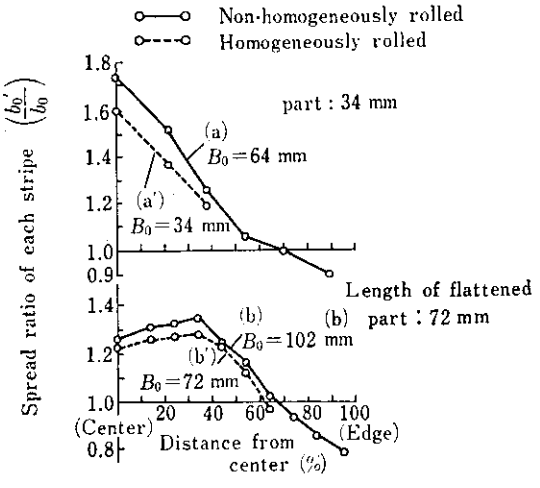

Fig. 5 Spread ratio destribution in transverse direction at midsection of plasticine models shown in Photo. 1

(a) B_0=64, Length of flattened part 34

(a′) B_0=34

(b) B_0=102, Length of flattened part 72

(b′) B_0=72

(a), (b) : Non-homogeneously rolled
(a′), (b′) : Homogeneously rolled
H_0=40, H_1=24 Unit : mm

Photo. 1 Spread pattern of plasticine models deformed by the rolls shown in Fig. 4 in comparison with flat rolled ones (a′) (b′)

rolled; while a noticeable width contraction occurs at both ends of a light reduction. This shows that a constraint force works at the central flat portion, counteracting the elongation from both ends to the rolling direction. This phenomenon gives us an important clue in studying the spread in the case of non-homogeneous rolling. **Fig. 6** shows the result of investigation of the changes of external dimensions of the material that was stopped rolling halfway when the ends were freed from the roll force. The arrows in the figure indicate the rolling direction, the horizontal axis represents the positions in the longitudinal direction of the rolled material, indicator No. 20 is the roll contact starting point, and No. 16 is the roll center.

In this figure, changes in the elongation coefficient (λ_w) in the rolling direction, maximum spread ratio (B_0'/B_0), flange width reduction ratio (F_0'/F_0), spread ratio on the web surface (b_0'/b_0) and the plate thickness in the center (H_1) are shown in their respective positions. It is clear from this figure that a great spread had already been caused in the material immediately before it came into contact with the roll, in addition that the plate thickness recovered, causing a spread, after the material had passed through the roll center. As these deformations can be recognized in areas Ⓐ and Ⓑ in the figure, they shall hereinafter be referred to as pre- and post-rolling deformation, respectively.

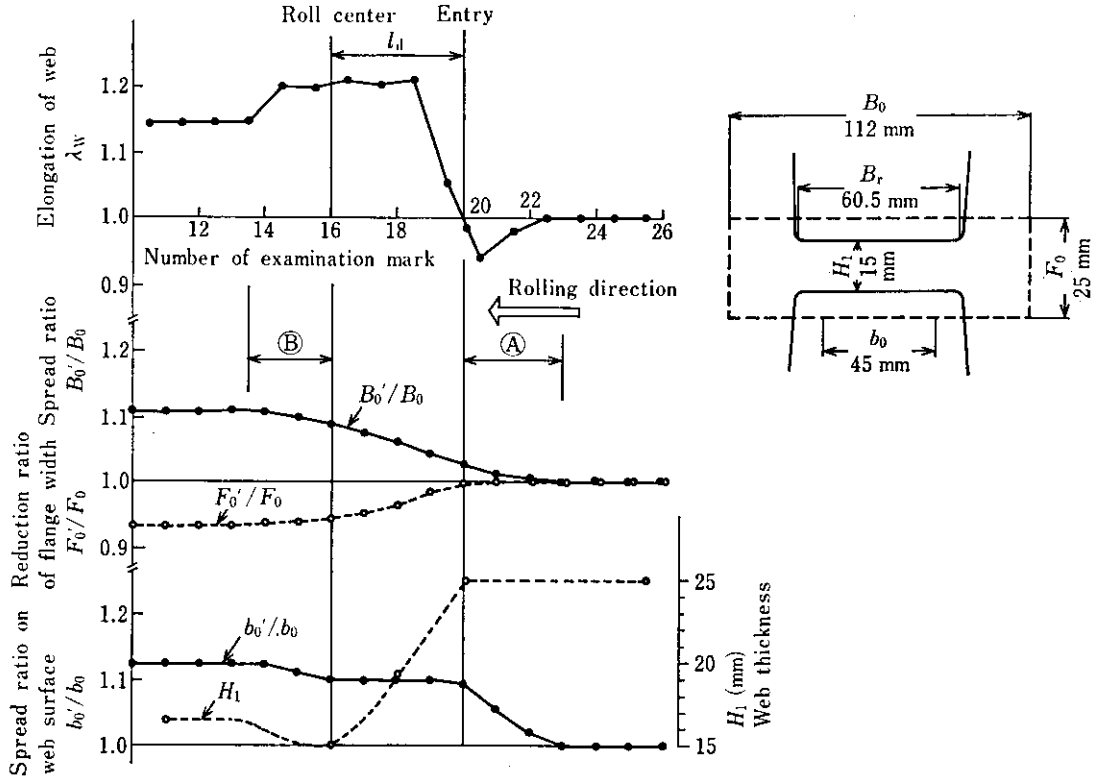

Fig. 6 Distribution of elongation coefficient, spread ratio, flange width reduction ratio and web thickness in rolling direction obtained with incompletely rolled plasticine model deformed only in center part of the plate

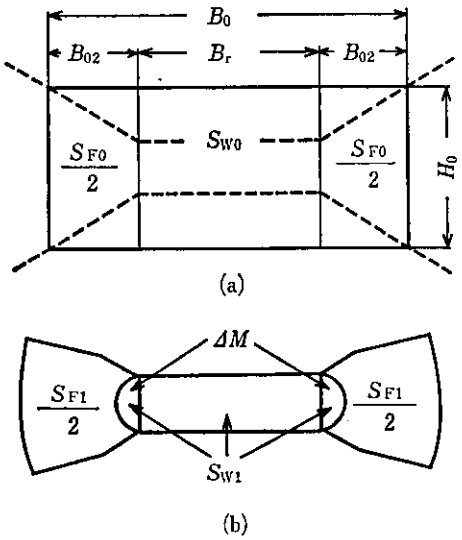

Fig. 7 Cross sections of specimen before (a) and after (b) non-homogeneous rolling in transverse direction (dotted lines show pass rolls)

3.2 Metal Flow Equation

The shapes of the cross section before and after rolling are defined as shown in **Fig. 7**. When the elongation coefficient after rolling is represented by λ and it is assumed that metal flow ΔM is caused as much as from flattened part B_r to both end parts under light reduction force, the following equation applies from the law of volume constancy:

$$\Delta M = \frac{H_0 \cdot B_r}{\lambda} - H_1 \cdot B_r \cdots\cdots\cdots\cdots\cdots (7)$$

If the elongation coefficient is given, the amount of metal flow can be derived from this, and on the contrary, if the amount of metal flow is produced, the elongation after rolling can be derived and therefore the sectional area can be obtained. In other words, the key point for estimating the external dimensions after rolling is to obtain the amount of metal flow.

The amount of metal flow from this flattened part is divided into three elements, as shown in **Fig. 8**, and represented by eq. **(8)**.

$$\Delta M = \Delta M_1 + \Delta M_2 - \Delta M_3 \cdots\cdots\cdots (8)$$

ΔM_1: The amount of metal flow when the plate of $B_r \times H_0$ is flattened to the thickness of H_1. It is calculated from eq. **(5)** or **(6)**.

ΔM_2: The sum of the amount of metal flow caused by the elongation constraint due to the existence of the light reduction part at the ends and the amount of metal flow caused by the pre- and post-rolling deformation. It changes in accordance with the tapers at the roll ends.

ΔM_3: The amount of metal flow caused by rolling both end parts toward the center flattended part. When the end parts are converted by the mean height method for flat rolling, it is calculated from eq. **(5)** or **(6)**. It also changes in accordance with the tapers at the roll ends.

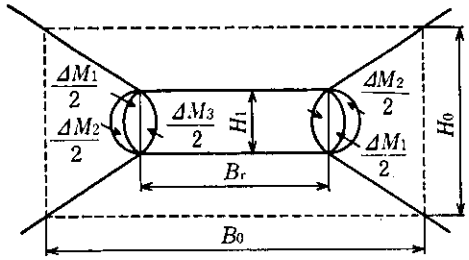

Fig. 8 Amount of metal flow (ΔM_1) between flat rolled part (S_{W0}) and taper rolled part (S_{F0}): ΔM_1 and ΔM_2 are metal flow from S_{W0} to S_{F0}, ΔM_3 from S_{F0} to S_{W0}

Therefore, though eq. **(8)** corresponding to the tapers of the roll is derived, it is changed as follows by referring to the metal flow at a particular taper angle:

$$\Delta M = \Delta M_1 + \alpha \Delta M'_2 - \beta \Delta M'_3 \cdots\cdots\cdots (9)$$

where $\Delta M'_2$ stands for the metal flow under the condition that the taper angle is 90°, that is, the ends are entirely free from reduction, and $\Delta M'_3$ stands for the metal flow when the end parts are converted by the mean height method for flat rolling (taper angle is 0°). In eq. **(9)**, α and β are constants that vary between 0 and 1 in accordance with the taper angle. As for $\Delta M'_2$, eq. **(10)** was obtained by the regression of the experimental data:

$$\Delta M'_2 = 1.29(S_{F0}/S_0)^{1.258} \times \left(\frac{\sqrt{R(H_0 - H_1)}}{B_r}\right)^{-0.27} \times (S_{F0}/S_0) \cdot B_r \times (H_0 - H_1) \cdots (10)$$

where S_0 stands for the sectional area of the material before rolling, and S_{F0} for the sectional area of the reduction-free (light reduction) part before rolling.

A number of materials having different shape factors were rolled by a roll having tapers of 8/15 at the end parts. By multiple regression analysis of the results,

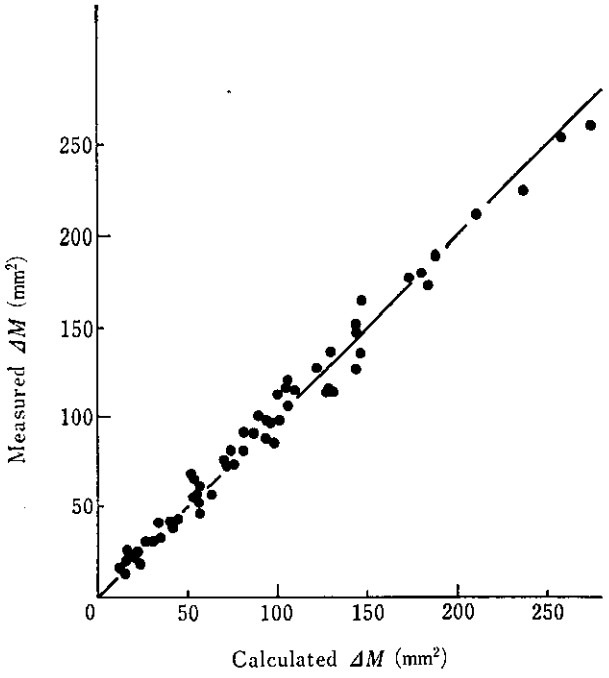

Fig. 9 Comparison between calculated and measured ΔM in plate non-homogeneously rolled in transverse direction

α and β were determined, and eq. **(11)** was obtained:

$$\Delta M = \Delta M_1 + 0.72\Delta M'_2 - 0.141\Delta M'_3 = \Delta M_1 + \Delta M_2 - \Delta M_3 \cdots\cdots\cdots\cdots (11)$$

This equation can be regarded as the metal flow expression corresponding to a particular roll shape. When the calculated values by eq. **(11)** and the measured values are compared with each other by varying rolling conditions, both coincide well with each other as shown in **Fig. 9**, and thus, the accuracy of this expression can be assured.

3.3 Verification of Validity of Metal Flow Equation

The deformations of plate materials having sectional dimensions of $B_0 \times H_0$ were calculated and compared with one another by each metal flow equation for the above-mentioned flat rolling and transverse direction non-homogeneous rolling. That is, the elongation coefficient λ_T in the case of flat rolling where the plate is rolled to the thickness of H_1 is derived from eq. **(12)**. (For the symbols used, refer to **Fig. 1**.)

$$\lambda_T = \frac{H_0 \cdot B_0}{H_1 \cdot B_{1m}} = \frac{H_0 \cdot B_0}{\Delta M_1 + H_1 \cdot B_0} \cdots\cdots\cdots (12)$$

In non-homogeneous rolling, on the other hand, the width is divided, as shown in **Fig. 10**, into three parts of B_r in the center and B_{02} at both ends, and both ends are dealt with as light reduction parts. Since the taper angle at the roll end parts is 0°, α is 0 and β is 1 in eq.

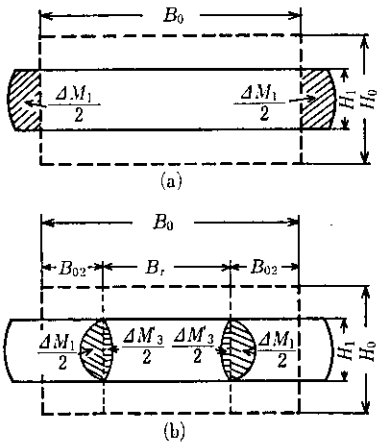

Fig. 10 Two models for calculating elongation coefficient in flat rolling (a) and (b), corresponding to equations (5) and (9), respectively

(9), so that the amount of metal flow from the center part (part B_r) to the end parts is, after all:

$$\Delta M = \Delta M_1 - \Delta M'_3 \cdots\cdots\cdots\cdots (13)$$

Therefore, the elongation coefficient λ_D when non-homogeneous rolling is assumed can be derived from eq. **(14)**:

$$\lambda_D = \frac{H_0 \cdot B_r}{(\Delta M_1 - \Delta M'_3) + H_1 \cdot B_r} \cdots\cdots\cdots (14)$$

when λ_T and λ_D are calculated and compared with each other with the rolling condition varied, both coincide well with each other, as shown in **Fig. 11**, and it turns out, as shown in **Fig. 8**, that it is valid to obtain the metal flow by dividing into 3 elements and then summing them.

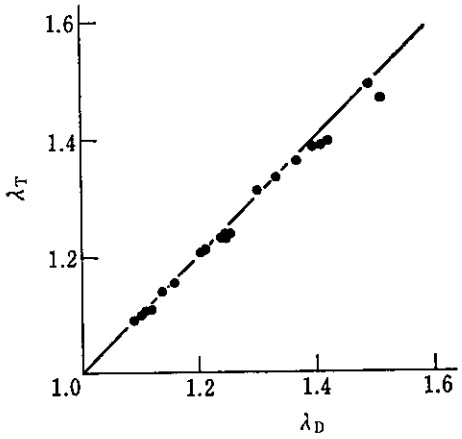

Fig. 11 Comparison in calculated elongation coefficients between equations (5) and (9)

4 Metal Flow Equation when Web of Dog Bone is Individually Rolled

Taking a dog bone which is made up of web and flange, rolling was performed only on the web, and its deformation behavior was studied. It was assumed that the part flattened by the roll was of three lengths (B_r): 38.5, 60.5, and 98.5 mm, with the flange completely free from any roll force during the deformation of the web.

4.1 Characteristic Deformation Behavior

Fig. 12 shows the distribution of spread ratio on the cross section when the plasticine material having a stripe pattern on the cross section was subjected to a 40% reduction. Three kinds of materials were rolled for each roll shape: a dog bone, (virtually a plate) of which flange leg length is 0, and a plate corresponding to the web of a dog bone. (In the dog bone, the area of the flange was constant.) It is clear from this figure that the larger the area of reduction-free part at the end in the transverse direction is, the larger the spread in the reduction part, and also that transverse contraction is caused, on the contrary, in the reduction-free part and above all, in the end part of material C-2 of which shape factor is large and reduction-free area is small, and noticeable transverse contraction is caused. In addition, it is evident that the position which will be the peak of the spread ratio in correspondence to the increase of the unflattened area and the amount of deformation before rolling shifts toward the center of the width.

Fig. 13 shows the result of the investigation on the change of the external dimensions sequentially from the incoming side to the outgoing side, with materials B-1, B-2 and B-3 in **Fig. 12** stopped before completion of rolling. The points at which it differs in particular from the deformation behavior of plate rolling material (B-1) can be classified as follows according to positions:

(1) Deformation up to the roll entry
In the rolling material having a roll force-free part, the distance between indication marks on the web surface expands in the transverse direction due to the transverse spread caused from a roll force part, and the plate enters the rolls in such a way that the web height and the internal web width have increased. In addition to this, a large deformation before rolling is apparent, as the web surfaces is contracted in the rolling direction. The larger the sectional area ratio (S_{F0}/F_0) of the overall section to the roll force-free part, the larger the amount of pre-rolling deformation. Moreover, the larger S_{F0}/F_0 and B_r, the larger the area of pre-rolling deformation.

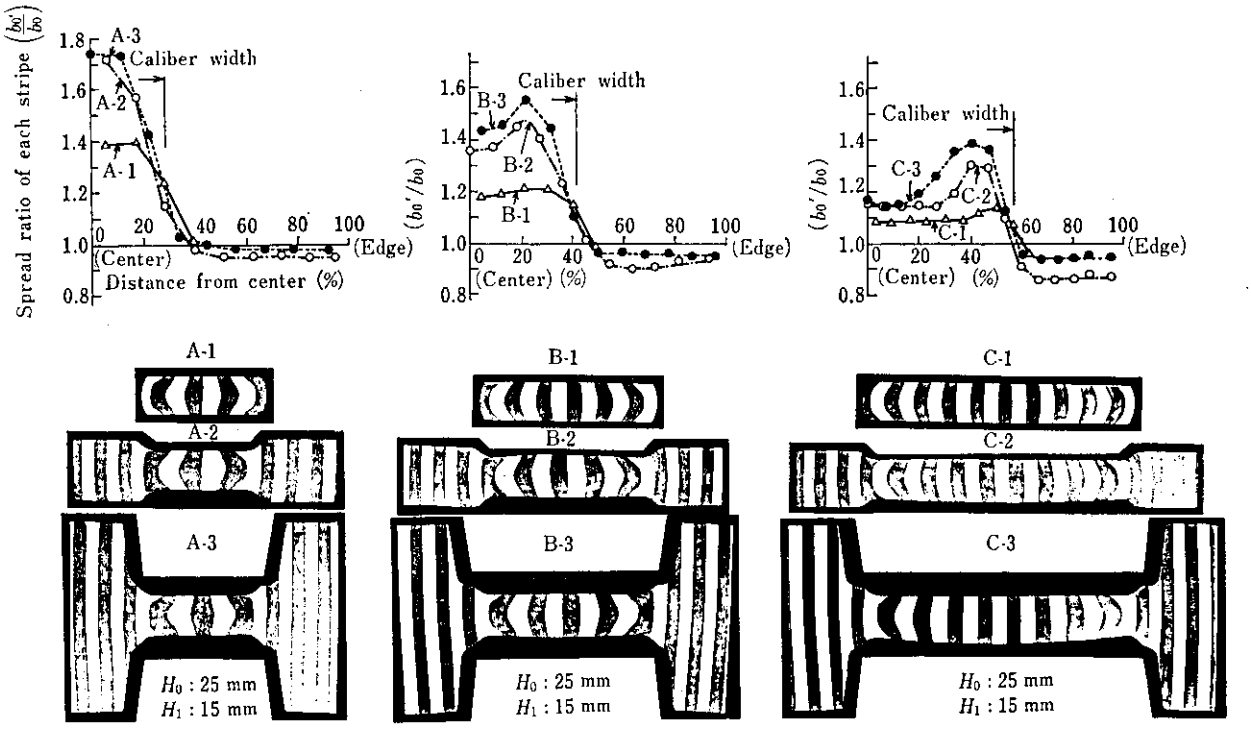

Fig. 12 Spread pattern and distribution in transverse direction of beam blanks with different web height after rolling only web part as compared with plates

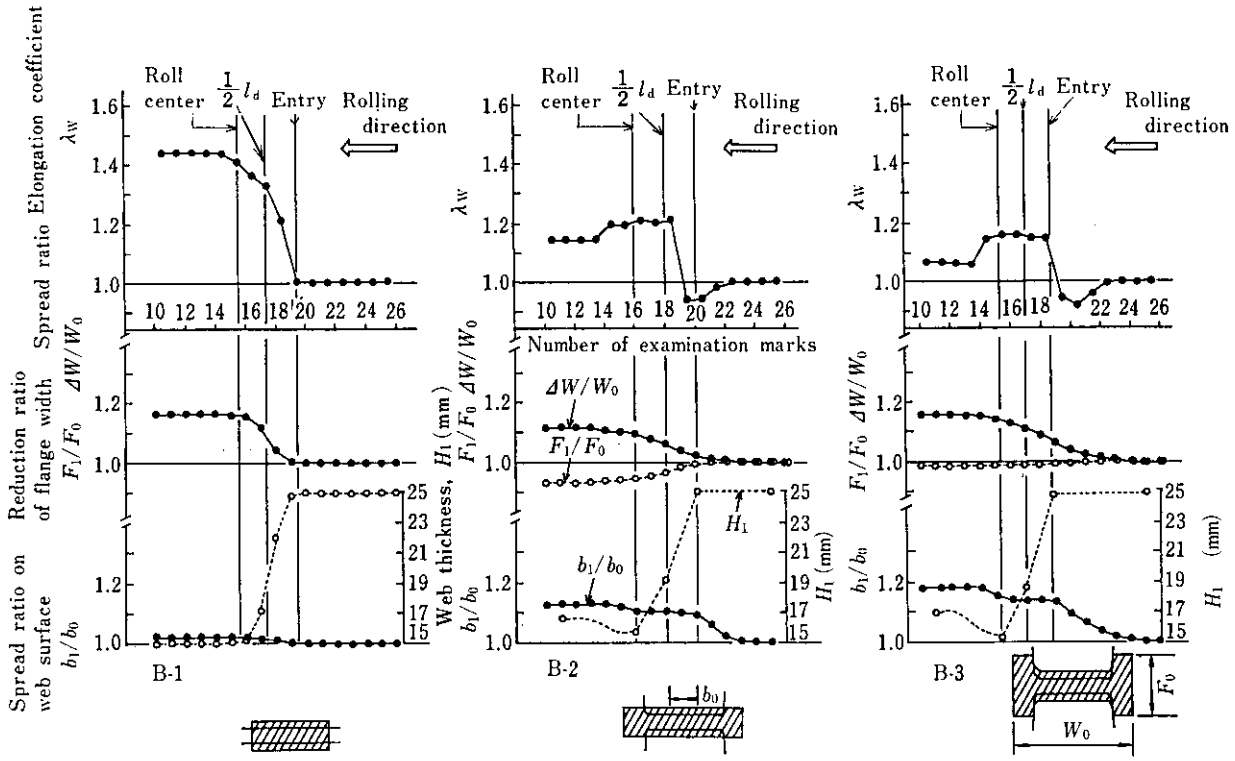

Fig. 13 Distribution of elongation coefficient, spread ratio, flange width reduction ratio, and web thickness in rolling direction, obtained with incompletely rolled beam blanks deformed only in web part

(2) Deformation from roll entry to roll center
Although the web starts its elongation, the elongation does not uniformly increase up to the roll center, beginning with 0, as in the case of flat plate rolling material, but under the elongation constraint from the unflattened part, elongation stops increasing at approximately 1/2 of the projected contact length, starting from contraction. The smaller S_{F0}/S_0 is and the larger B_r is, the larger the elongation coefficient, (Refer to **Fig. 12.**) The indicator marks on the web surface do not spread, and the contact surface with the roll is nearly sticking. However, while the spread is still caused by the web rolling, the increase of the web height equals to the amount of elongation-induced contraction in the roll force-free part subtracted from the amount of the the web spread. Most decrease of the flange width is caused in this area.

(3) Deformation after passing through roll center
The web forcibly elongated in the rolling direction under the constraint of the roll force-free part within the roll bite is contracted in the rolling direction by the contractive internal stress acting in this area. At the same time, it increases its thickness and spreads in deformation, and a noticeable post-rolling deformation is seen. The amount of this deformation and the influence of S_{F0}/S_0 and B_r upon the length of the deformation area are same as those in the case of (1).

4.2 Metal Flow Equation and External Dimensions Estimating Equation

The amount of the metal flow (the sectional area shifted from the part under roll force toward the flanges) caused by the progress in the rolling process is produced by closely observing the changes of the sectional area of the dog bone having a stripe pattern at such stages as its contact point with the roll, in the roll center and after rolling, respectively.

Fig. 14 is a stage-by-stage indication of metal flow amount after the web only rolling performed in the

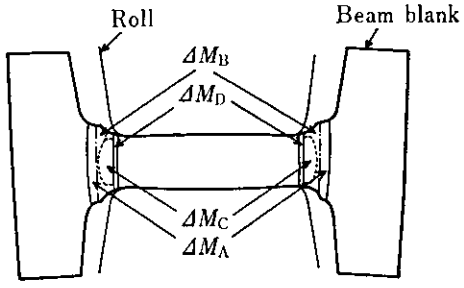

Fig. 14 Distinction of metal flows arisen by different causes

above manner. The amount of metal flow at each deformation stage is expressed as part of the total metal flow. ΔM_A stands for the amount of metal flow by pre-rolling deformation, ΔM_D by post-rolling deformation, and the rest is the amount of metal flow caused within the roll bite. This is further divided into the amount of metal flow ΔM_C when the web is rolled regarded as a flat plate (the results in flat rolling are used) and the residual ΔM_B. This ΔM_B comes into being by the constraint given by the roll force-free part to the elongation of the part under roll force.

Therefore, according to the preceding chapter, ΔM_1, ΔM_2 and ΔM_3 in eq. **(9)** are $\Delta M_1 = \Delta M_C$, $\Delta M_2 = \Delta M_A + \Delta M_B + \Delta M_D$ and $\Delta M_3 = 0$, respectively, and the following metal flow equation is obtained:

$$\Delta M = \Delta M_1 + \Delta M_2 \quad \cdots\cdots\cdots\cdots (15)$$
$$\Delta M_2 = \Delta M_2'$$

The material of which S_{F0}/S_0 was widely changed was rolled on rolls of which B_r was 38.5 mm, 60.5 mm and 98.5 mm, respectively, so that the rolling reduction of the web might be within the 10%–40% range, and the validity of eq. **(15)** was investigated. **Fig. 15** shows the relationship between the calculated values and the measured values, which correspond well with each other. Thus, it is clear that the metal flow equation is sufficiently applicable to the web only rolling of the dog bone. If the amount of metal flow is obtained, the elongation after rolling as well as the sectional area will be derived, therby facilitating the calculation of external dimensions from both these and the shape of deformation.

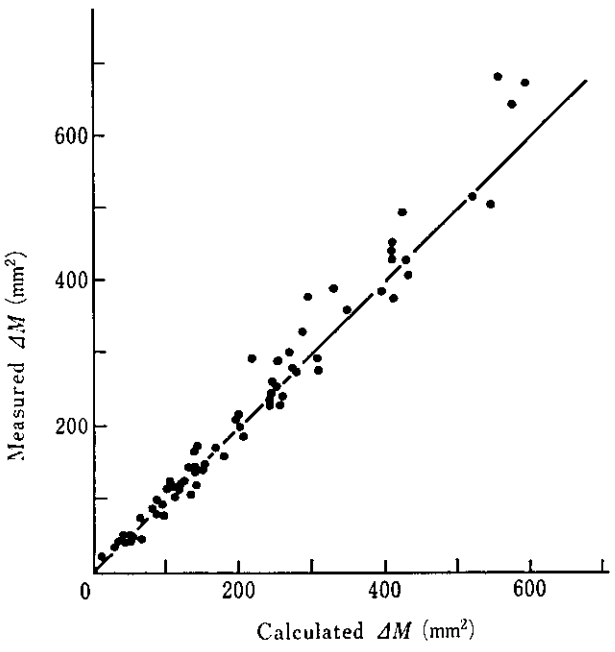

Fig. 15 Comparison between calculated and measured ΔM during rolling only web part of beam blank

The shape estimating equation by the method of rolling only the web of the dog bone is as follows:

(1) Metal flow equation

$$\Delta M = \Delta M_1 + \Delta M_2 \quad \cdots\cdots\cdots\cdots (15)$$

(2) Elongation estimating equation

$$\lambda = \frac{H_0 \cdot B_r}{\Delta M + H_1 \cdot B_r} \quad \cdots\cdots\cdots\cdots (16)$$

(3) Post-rolling sectional area estimating equation

$$S_1 = S_0/\lambda \quad \cdots\cdots\cdots\cdots (17)$$

(4) Web height estimating equation

$$W_1 = B_r + (W_0 - B_r)/\sqrt{\lambda} + 2.18\Delta M/(H_0/\sqrt{\lambda} + H_1) \quad \cdots (18)$$

(5) Flange width estimating equation

$$F_1 = F_0/\{1 + 0.73(\sqrt{\lambda} - 1)\} \quad \cdots\cdots\cdots (19)$$

(6) Web thickness estimating equation

$$H_1 = H_1^* + 0.107H_0(S_{F0}/S_0)^{1.151} \times \left(\frac{H_0 - H_1^*}{H_0}\right)^{0.351} \times \left(\frac{B_r}{H_0}\right)^{1.246} \quad \cdots (20)$$

S_1: Sectional area after rolling
W_0, W_1: Web heights before and after rolling
F_0, F_1: Flange widths before and after rolling
H_1^*: Roll gap during rolling

4.3 Deformation Behavior when Web of Dog Bone Having Different Web Heights are Rolled

The deformation behavior was examined by applying the above-mentioned model equation to the only web rolling of the dog bones for H300 × 300 – H900 × 300 of which flange section area consisted of two exclusive types (S_{F0}: 92 640 mm² and 27 240 mm²). The width (B_r) of the roll corresponding to each size of the H-shape steel was determined, as shown in **Table 1**, referring to the actual steel. Rolling of 4 passes in total was carried out as to the thickness from 120 mm to 40 mm so that 1 pass might be the rolling reduction of 20 mm, with the dog bone as shown in **Fig. 16** as the initial cross section. In addition to this, the roll radius of $R = 625$ mm was assumed.

In **Figs. 17** and **18**, the results of calculation of the change in elongation coefficient, flange width and web height, resulting from the rolling were shown as to H300 × 300 and H900 × 300 in **Table 1**.

Fig. 17 shows the case of a large sectional area of

the flange section. In rolling for H300 × 300 whose S_{F0}/S_0 is especially large, above all, no elongation is caused by rolling in the rolling direction because of the large amount of metal flow toward the flange but deformation is merely a spread in the transverse direction. Also, in H900 × 300 whose shape factor of the web is large, the elongation coefficient is as small as 1.32. The larger the web height, the larger the absolute value of the increment of the web height. And S_{F0}/S_0 increases with the progress of passes. Therefore, the elongation coefficient λ for each pass also decreases. Mark Δ of H300 × 300 in the figure shows the data of actual steel, and it is clear that the data coincide well with the results of calculation.

Fig. 18 shows the case where the flange cross section is small (hence, S_{F0}/S_0 is also small) and elongation constraint does not act so much. In this case, spread is little, and a marked elongation is caused. It is only in H300 × 300 that the elongation for each pass decreases with the progress of rolling. In the others, it increases gradually, and this tendency is more noticeable, the larger the web height is. The flange width greatly decreases with the elongation, and especially

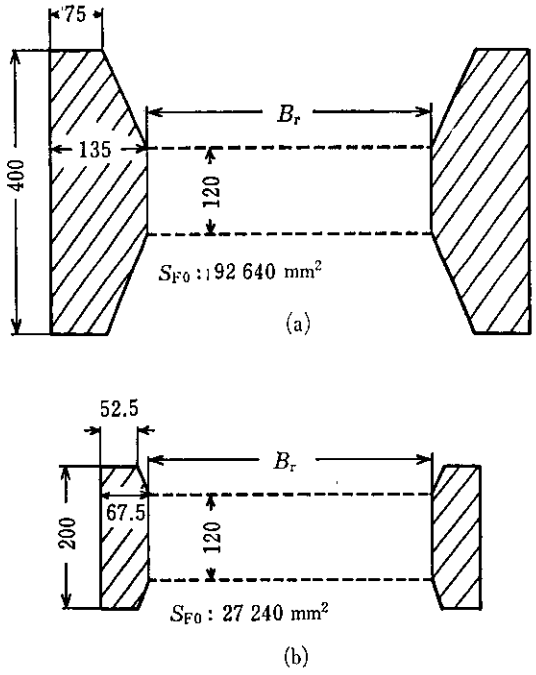

Fig. 16 Dimensions of two beam blanks with different flange area for the calculation of metal flow

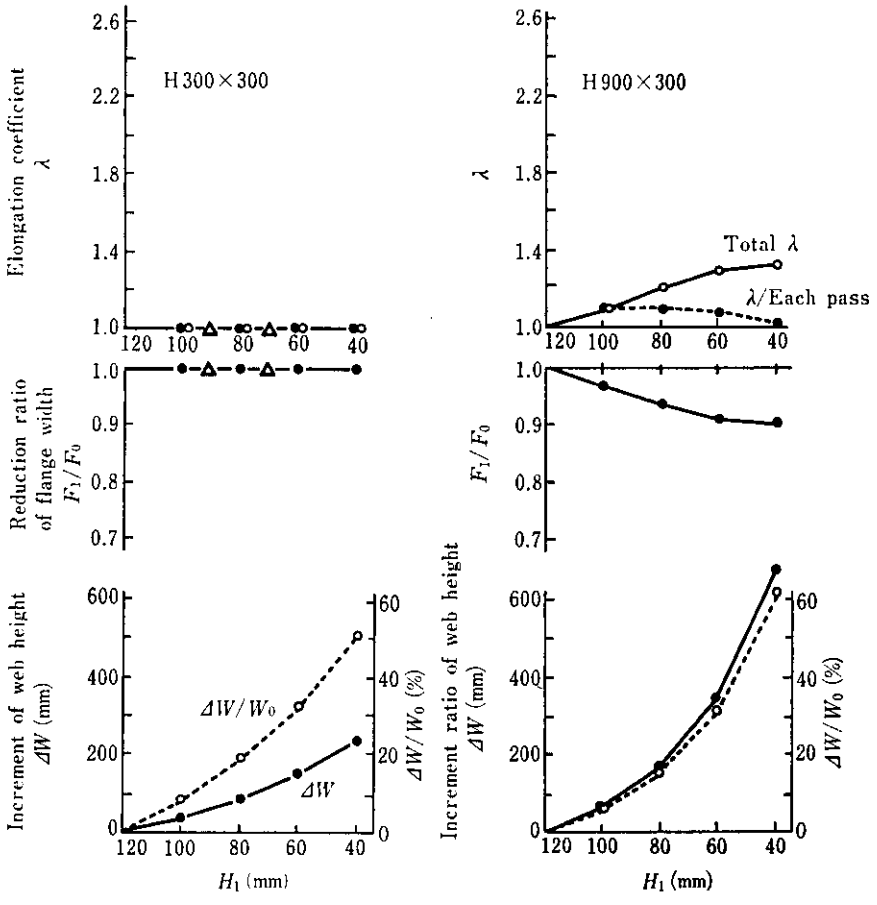

Fig. 17 Calculated deformation behavior of the beam blanks with initial dimensions shown in Fig. 16 (a) during rolling only web part

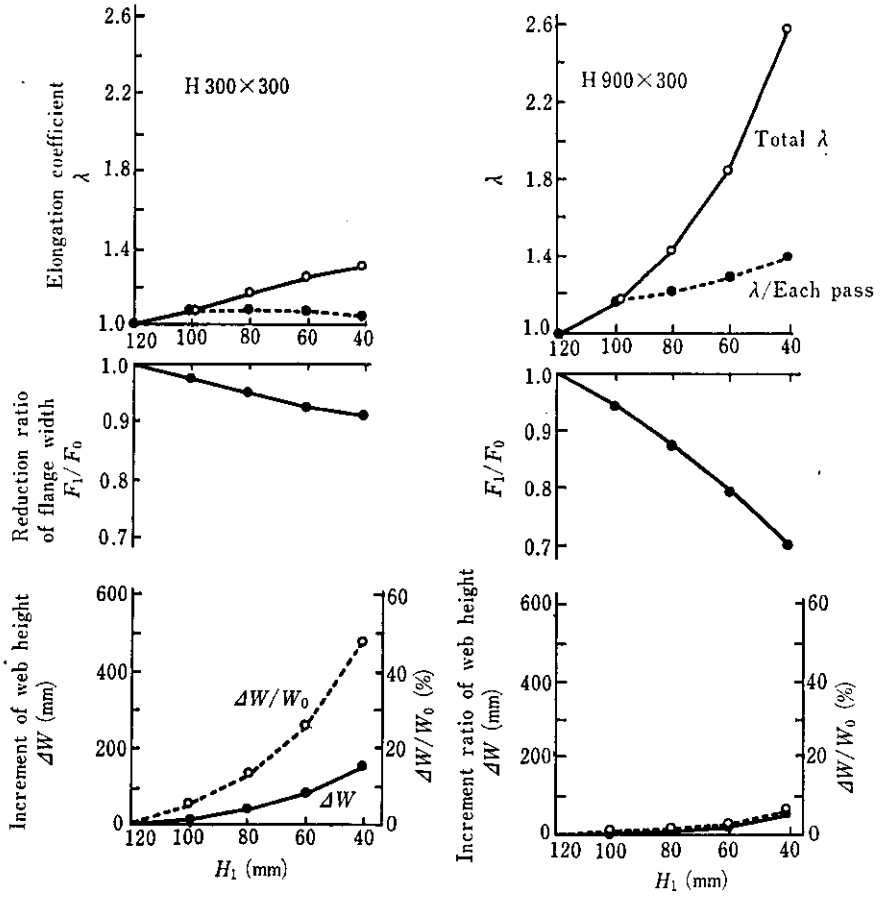

Fig. 18 Calculated deformation behavior of the beam blanks with initial dimensions shown in Fig. 16 (b) during rolling only web part

Table 1 Beam blank size and length of flattened part (B_r) in pass rolls

Beam blank size	H300×300	H400×300	H500×300	H600×300	H700×300	H800×300	H900×300
B_r of roll (mm)	200	300	410	510	610	730	830

in H900 × 300, it decreases to 70% of the width before rolling. The increment of the web height becomes less, the larger the web height, contrary to **Fig. 17**. **Fig. 19** shows the comparison between the increment ratios of the web height ($\Delta W/W_0$) of material (a) in **Fig. 16** according to sizes. It illustrates how effectively the web height can be extended for the rolling reduction of 20 mm in each pass. It is clear from this that, H400 × 300 in the state where the web thickness is reduced from 120 mm to 80 mm, H500 × 300 for a thickness up to 60 mm and H600 × 300 for a thickness up to 40 mm have the maximum spread ratio.

4.4 Application of Model Equations to Partial Web Rolling Method

As is clear from **Figs. 17** and **18**, the elongation in the rolling direction increases in the case of a large web height even if only the web is rolled, and as a result an inevitable shortages tends to occur to flange sectional area.

In ordinary pass rolling, deformation due to rolling is more liable to occur in elongation since spread is constrained, so that a noticeable decrease in flange sectional area is caused. It is a very important forming technique in breakdown rolling to suppress elongation

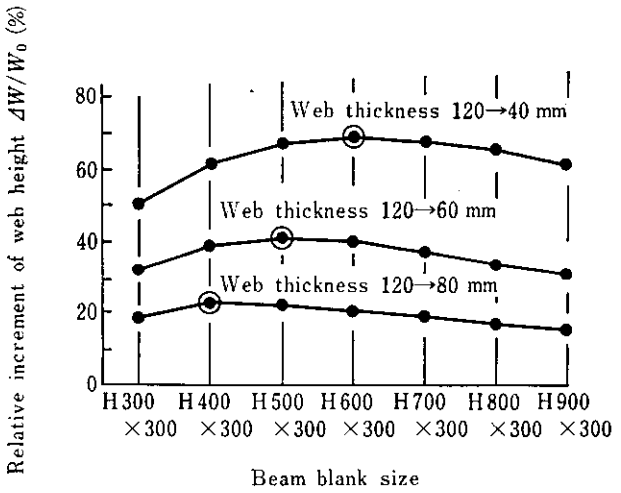

Fig. 19 Change in relative increment of web height with size in the case of beam blanks shown in Fig. 16 (a) and amount of reduction by rolling only web part

and avoid a decrease in the sectional area of the flange section. For this purpose, ΔM in eq. **(16)**, namely ΔM_1 and ΔM_2 have to be increased. As is clear from eq. **(10)**, S_{F0}/S_0 has the largest influence upon ΔM_2, and it must be increased. One of the effective methods of increasing S_{F0}/S_0 is to decrease B_r, and by doing this, further effect can be obtained since ΔM_1 can also be increased at the same time.

Therefore, even in the case of a size whose internal width of the web is large, if the web is rolled by dividing it by rolls whose rolling width is small, the thickness of the web can be decreased in a state where elongation is little, and thus, effective flange forming rolling can be carried out while maintaining the sectional area of the flange.

The partial web rolling method was devised on the basis of this idea. It is the method which repeats rolling only the web (b) where B_r is small and flange forming rolling alternately, as shown in **Fig. 20**.

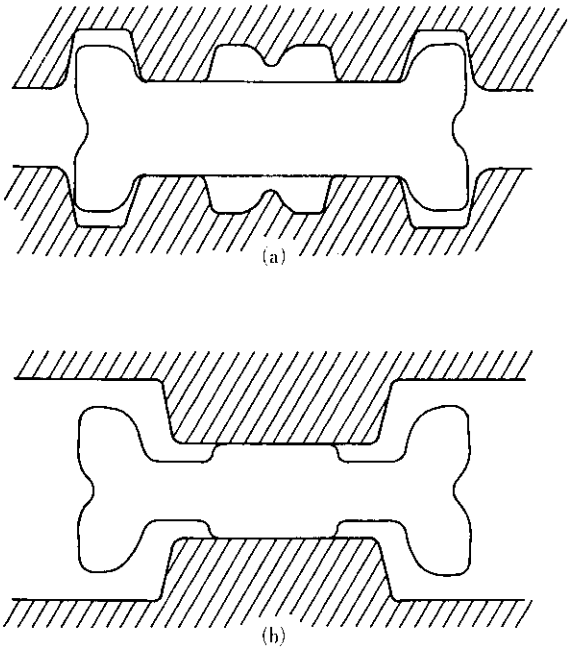

Fig. 20 Schema of partial-web rolling with (a) and (b) type passes repeated

Since B_r increases during rolling in the deformation in **Fig. 20** (b), the conventional model expressions should be modified more or less in consideration of this fact. **Fig. 21** illustrates as example of the shape of the cross section of a pass during partial web rolling in actual steel. The estimated value and measured value of the flange width in this deformation coincide well with each other, as shown in **Table 2**. In addition to this, estimation of the web height is possible.

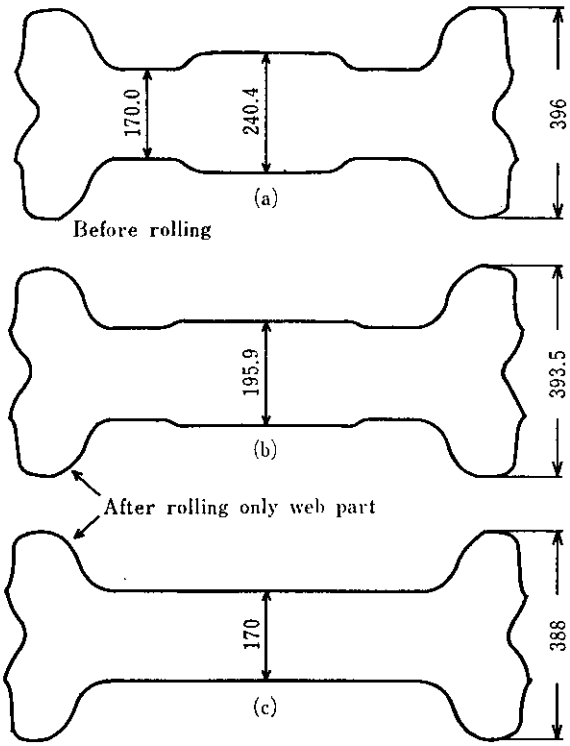

Fig. 21 Shapes and dimensions of beam blanks obtained by partial web rolling

Table 2 Comparison in flange width between calculation and measurement obtained by rolling only web part of beam blank, using hot steel

	Web center thickness (mm)	Measured flange width(mm)	Calculated flange width(mm)
Before rolling	240.4	396.0	396.0
After rolling	195.9	393.5	392.4
	170.0	388.0	390.8

As described above, it has become possible to determine optimum rolling conditions involving pass shape, material shape, rolling reduction, etc; by making the most of the model expression for the deformation behavior based on the metal flow equation, without using actual steel.

5 Conclusion

The authors took note of web rolling as having the greatest influence upon the deformation of the dog bone material for H-shape in the open pass rolling, and performed experiments with plasticine models. At first, the case where the web is regarded as a flat plate, and then the case where only the web of the dog bone is rolled, were analyzed and the following results were obtained.

(1) The basis of the amount of deformation is the amount of metal flow, and in the case of plate rolling, the experimental expressions for calculating them according to rolling conditions were prepared in accordance with each of single barrel deformation and double bulge deformation.

(2) The amount of metal flow ΔM from a heavy roll force part to a light roll force part in rolling a plate in the transverse direction by non-homogeneous force can be obtained, as follows:

$$\Delta M = \Delta M_1 + \Delta M_2 - \Delta M_3$$

In the above equation, ΔM_1 is the amount of metal flow when the heavy roll force part is regarded as a flat plate, ΔM_2 is the amount of metal flow caused when the light roll force part constrains the elongation in the rolling direction, and ΔM_3 is the amount of metal flow by the rolling of the light roll force part, respectively. All of them can be quantified.

(3) In rolling only the web of the dog bone, a marked spread deformation is caused before and after contact with the roll, and it becomes more noticeable, the larger the flange cross section. The amount of metal flow in this case is described as follows:

$$\Delta M = \Delta M_1 + \Delta M_2$$

(4) The amount thus obtained can be used as the basis for, calculating the dimensions of material after rolling.

(5) The prepared calculation expressions have high accuracy, and they can be suitably applied to the estimation of deformation in actual steel rolling.

(6) By the examination described above, the rolling conditions that will result in little elongation and large spread can be obtained, leading to the development of the partial web rolling method effective for rolling large cross section H-shape steel from slabs.

References

1) T. Kusaba and T. Sasaki: *Kawasaki Steel Technical Report*, **11** (1979) 4, p. 485 (in Japanese)

2) T. Kusaba and T. Sasaki: *The Proceedings of the 31st Japanese Joint Conference for the Technology of Plasticity* (1980), p. 411

3) T. Tanaka, M. Yamashita, K. Hitomi, T. Ehiro, T. Akune, and T. Kusaba: *Kawasaki Steel Technical Report*, **10** (1979) 4, p. 69 (in Japanese)

4) S. Yanagimoto: *Journal of the Japan Society for Technology of Plasticity*, **5** (1964) 40, p. 315

5) T. Yanazawa, T. Tanaka, M. Yamashita, H. Okumura and T. Kusaba: *Kawasaki Steel Giho*, **13** (1981) 3, p. 1